Available online at www.sciencedirect.com

ScienceDirect

Defence Technology ■■ (2016) ■■–■■

www.elsevier.com/locate/dt

Transient out-of-plane distortion of multi-pass fillet welded tube to pipe T-joints

R. VETRISELVAN [a,*], K. DEVAKUMARAN [a], P. SATHIYA [b], G. RAVICHANDRAN [a]

[a] *Welding Research Institute, Tiruchirappalli 620014, India*

[b] *National Institute of Technology, Tiruchirappalli 620015, India*

Received 5 February 2016; revised 30 May 2016; accepted 12 June 2016

Available online

Abstract

The out-of-plane distortion induced in a multi-pass circumferential fillet welding of tube to pipe under different weld sequences and directions was studied using Finite Element Method (FEM) based Sysweld software and verified experimentally. The FEM analyses consisted of thermal and mechanical analyses. Thermal analysis was validated with experimental transient temperature measurements. In the mechanical analysis, three different weld sequences and directions were considered to understand the mechanism of out-of-plane distortion in the tube to pipe T-joints. It was learnt that the welding direction plays a major role in minimizing the out-of-plane distortion. Further, during circumferential fillet welding of the tube to pipe component, the out-of-plane distortion generated in the *x* direction was primarily influenced by heat input due to the start and stop points, whereas the distortion in the *z* direction was influenced by time lag and welding direction. The FEM predicted distortion was compared with experimental measurements and the mechanism of out-of-plane distortion was confirmed.

Keywords: Multi-pass welds; FEM; Temperature field; Out-of-plane distortion; tube to pipe T-joints; Circumferential welding

1. Introduction

Welded T-joints are one of the commonly used joint types. Often pipes and tubes are welded in perpendicular orientation constituting a T-joint. This is possible with circumferential welding. These circumferential fillet welded socket joints are widely used in various industries such as line pipes, automobiles, bridges, defense components, pressure vessels and structural applications. Owing to the relatively large wall thickness in certain tube to pipe systems, the fillet weld is often constructed with multiple weld passes. During the fabrication of these components welding induced distortion occurs.

T-joints experience out-of-plane distortion in both longitudinal and circumferential types of welding. Many authors have studied the distortion experienced due to longitudinal welding on a plate [1–6]. The temperature field of an arc and its mechanical effect on fillet welding of plates using FEM are also reported [6] and it was found that the arc start and stop points enhance the heat input and accordingly increase distortion in the case of longitudinal welding.

The out-of-plane distortion due to circumferential welding of thin-walled butt-welded pipes using FEM has been reported with the effect of weld thermal cycle on out-of-plane distortion generated under the different segment of the circumferential welding [7,8]. The buckling distortion is also another type of out-of-plane distortion experienced in case of thin cylindrical shells during circumferential welding [9,10]. Generally, out-of-plane distortion resulted in both longitudinal and circumferential fillet welding and this leads to misalignment, stress concentration, buckling and improper fit-up etc. However very few articles reported the out-of-plane distortion experienced during the circumferential welding of t-joints. The start and stop points have significant effect on out-of-plane distortion in the case of half-circumferential fillet welding in a T-joint configuration, and it has been reported that the stop points have more influence on out-of-plane distortion than the start points [11,12]. In the case of full circumferential welding, both the start and stop points merge with each other and the effect is not studied so far. It is inferred from the literature survey that transient analysis of the full circumferential multi-pass welding on a tube to pipe component in the t-joint orientation is not

Peer review under responsibility of China Ordnance Society.

* Corresponding author.

E-mail addresses: vetri@bheltry.co.in, vetriselvan2003@gmail.com (R. VETRISELVAN).

http://dx.doi.org/10.1016/j.dt.2016.06.002

Please cite this article in press as: R. Vetriselvan, K. Devakumaran, P. Sathiya, G. Ravichandran, Transient out-of-plane distortion of multi-pass fillet welded tube to pipe T-joints, Defence Technology (2016), doi: 10.1016/j.dt.2016.06.002

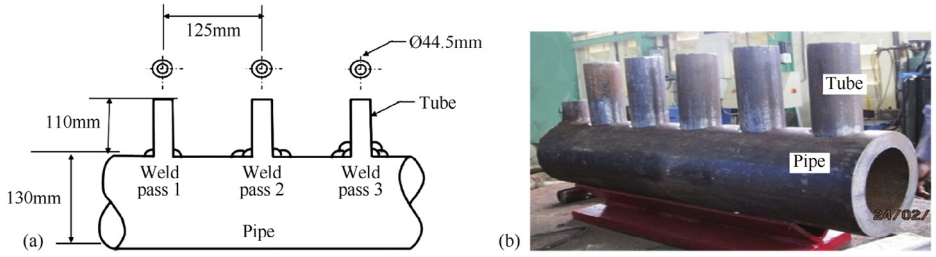

Fig. 1. The schematic diagram and the photographic view of the tube to pipe arrangement.

available either experimentally or by other modes such as FEM simulation. These data, when made available, are of vital importance for various industrial and defense applications.

Thus, the present work describes the out-of-plane distortion generated in multi-pass full circumferential fillet welding of tube to pipe under different weld sequences and directions. The studies were carried out using FEM based Sysweld [13] software. Firstly, the thermal analysis of the FEM model for the tube to pipe welding was carried out followed by mechanical analysis. In the mechanical analysis, three different weld sequences and directions were considered to understand the mechanism of out-of-plane distortion in the tube to pipe welding. Further, the predicted FEM model was verified experimentally. Based on the FEM and experimental results, the suitable welding procedure was explored for the tube to pipe fabrication.

2. Experimentation

The welding arrangement considered for the out-of-plane distortion analysis included the thick walled pipe consisting of lots of small tubes welded with the pipe. The schematic diagram and photographic view of the pipe and tube are shown in Fig. 1(a) and (b) respectively. The thickness and outer diameter of the pipe is 20 mm and 130 mm. The thickness and outer diameter of the tube are 5 mm and 44.5 mm. The material used for pipe and tube are low carbon steel of grade EN S355J2G3. The chemical composition of the material is given in Table 1. The multiple numbers of tubes are fillet welded using Shielded Metal Arc Welding (SMAW) process and multi-pass welding procedure used for the fillet welding of the tube to pipe component. Prior to welding, holes are drilled in the pipe and the tubes are inserted into it. The joint type is set on type and is shown schematically in Fig. 2(a).

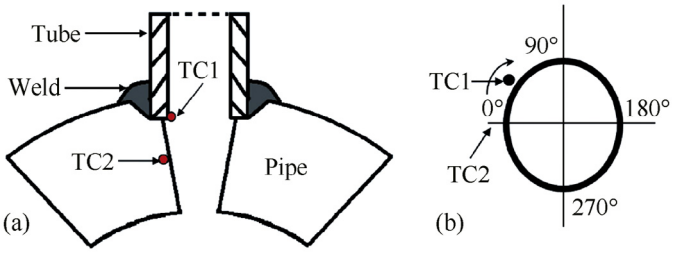

Fig. 2. The schematic diagram of set on type joint used in the tube to pipe welding.

2.1. Welding

The tubes are inserted into the holes in the pipe and it is tack welded. After that, the tubes are aligned with the pipe's central axis using a standard jig. Three weld sequences in reference to the start and stop points of welding direction were considered for the tube to pipe fabrication. The welding parameters used in the experimentation are given in Table 2. The welding parameters such as welding current and arc voltage were recorded using digital meter fitted in the welding power source during welding.

2.2. Measurement of temperature during welding

The temperature was measured during the tube to pipe welding using a thermocouple. The temperature measurement requires thermocouples and a data acquisition card. Two thermocouples are positioned in the weld region as shown in schematic representation in Fig. 2(b). The K-type thermocouple was used to measure the transient temperature in the weld vicinity. One thermocouple was positioned near the tube (TC1, 5 mm from weld) and another was positioned nearer to the pipe (TC2, 15 mm from weld metal). The data logging frequency for the thermocouple was set to 600 Hz. A computer-controlled data logger was used to capture the transient temperature

Table 1
The chemical composition of the carbon steel used for the study.

Composition	C	Si	Mn	P	S
%	0.35	0.10	0.30	0.035	0.035

Table 2
The welding parameters used for tube to pipe fabrication.

Sl. no.	Welding parameters	
1	Welding current/A	160 for root pass 220 for subsequent weld passes
2	Arc voltage/V	23
3	Welding speed/(mm·s^{-1})	2
4	Electrode	E 7018, Φ 3.15 mm for root pass E 7018, Φ 4 mm for subsequent weld passes
5	Total number of weld passes considered for stub to header welding	3 (three)
6	Welding position	2F
7	Heat input/(kJ·mm^{-1}) ($\eta = 65\%$)	1.2 for root pass 1.65 for subsequent passes

Please cite this article in press as: R. Vetriselvan, K. Devakumaran, P. Sathiya, G. Ravichandran, Transient out-of-plane distortion of multi-pass fillet welded tube to pipe T-joints, Defence Technology (2016), doi: 10.1016/j.dt.2016.06.002

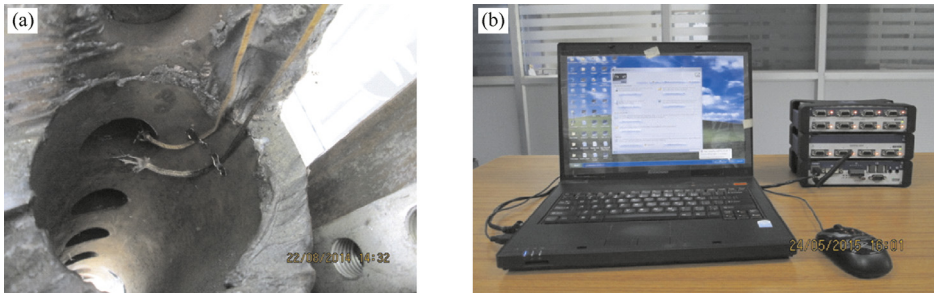

Fig. 3. (a) The photographic view of thermocouple on the tube to pipe component. (b) Data logger used during the study.

distribution during welding of the tube with pipe. The process of data logging was shielded against electrical interference. The temperature sensors and data logger instrument were calibrated before the experimental trial. Data logging was started before welding and the measurements were taken during first, second and third weld passes and until the distortion reached steady state values. Photographic view of the thermocouple on the tube to pipe set up with the data logger is shown in Fig. 3(a) and (b).

2.3. Measurement of out-of-plane distortion

The transient measurement of distortion of the tube during welding could not be measured as the length of the tube was only 110 mm and positioning displacement sensors at the end of the tube caused accessibility issues to the welder during all around circumferential welding. Hence, the out-of-plane distortion measurement was carried out using Vernier caliper after completion of every weld pass. Prior to welding of tube to pipe, the standard jig was mounted on the pipe to monitor the movement of the tube during circumferential weld deposition as shown in Fig. 4. The jig allows free movement of the tube in all the directions and enables the measurement of distortion from the initial position of the tube. The movement of the tube from its original position is referred to as out plane distortion in the tube to pipe fabrication. Under different weld sequences and weld directions, the out-of-plane distortion generated after welding (reached to room temperature) was measured using a Vernier-caliper having the least count of 0.02 mm.

3. Out-of-plane distortion analysis

3.1. Finite element model

The out-of-plane distortion generated during multi-pass fillet welding in the tube to pipe fabrication under different weld sequences was simulated. The material properties considered for the investigation are temperature dependent. The sizes of the pipe and the tube considered for FEM simulation are shown in Fig. 1(a). The tube to pipe model was meshed with solid elements. The meshed model consists of 25,000 nodes and 20,000 solid elements including tetrahedral and brick elements as shown in Fig. 5. The three weld passes were considered for the FEM analysis as shown in Fig. 6. FEM analysis of multipass weld deposition was carried out using element activation and deactivation technique [14]. The technique implies that the element is active until the temperature is dissipated to the surrounding through conduction, convection, and radiation when the heat is applied to the element. The death of the element will occur when the element reaches ambient temperature. The size of the finite element considered in the arc zone is about 2 mm and it increases away from the weld zone.

The isotropic elastic plastic approach was used for the analyses. The thermal analysis is based on the heat conduction formulation using temperature dependent thermophysical properties (Fig. 7(a)). The temperature dependent material properties considered for the mechanical investigation are shown in Fig. 7(b) [12]. The Goldak's non-axisymmetric 3D double ellipsoid heat source was considered for the transient thermal analysis of multipass weld deposition of the tube to pipe welding [15]. The arc heat source moves through the defined one-dimensional circumferential trajectory at a given welding speed. The present FEM model also includes the heat losses due to convection and radiation during welding. The ambient temperature of 25 °C was considered. The heat input is estimated as follows

$$Heat\ Input = \frac{V \times I}{S} \times \eta \tag{1}$$

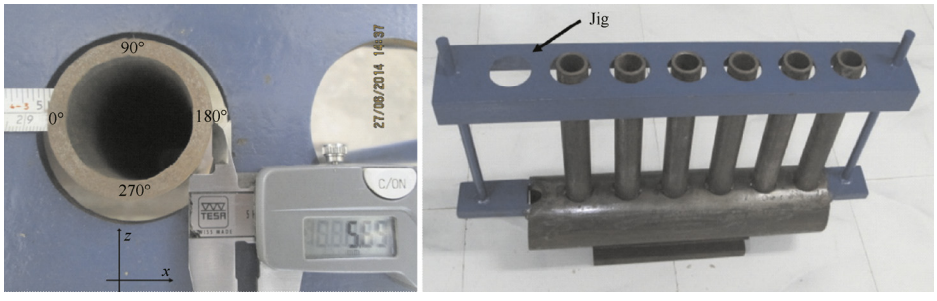

Fig. 4. The measurement of distortion using standard jig during tube to pipe welding.

Please cite this article in press as: R. Vetriselvan, K. Devakumaran, P. Sathiya, G. Ravichandran, Transient out-of-plane distortion of multi-pass fillet welded tube to pipe T-joints, Defence Technology (2016), doi: 10.1016/j.dt.2016.06.002

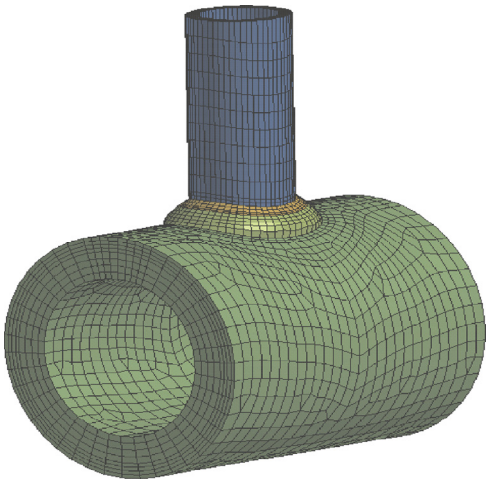

Fig. 5. The finite element model of a pipe with tube using solid elements.

where V is the arc voltage (volt), I is the welding current (ampere), S is the welding speed (mm·s^{-1}) and η is process efficiency 65 (%). The welding parameter used for the present investigation is given in Table 2. Based on the above considerations, the out-of-plane distortion generated on the tube to pipe fabrication during multi-pass weld deposition was simulated under three weld sequences in reference to the start and stop points as well as welding direction as shown schematically in Fig. 8. In addition, the clamping conditions contributed to the plastic stresses induced in the weldments. Hence, for the simulation, minimum clamping conditions were assumed to avoid the rigid body motion of the component. Three nodal points were rigidly clamped in the x, y, z directions. The clamping conditions considered for the simulation are shown in Fig. 9.

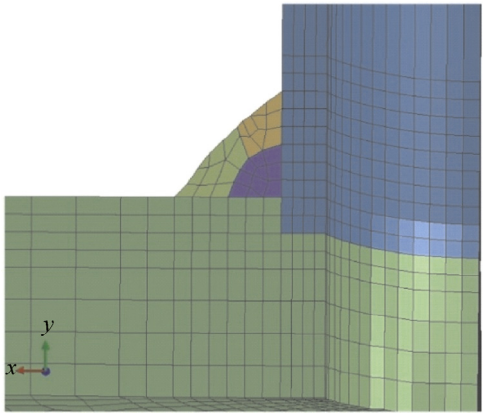

Fig. 6. The cross sectional view of three weld passes between tube and pipe.

The start and stop points of all three-weld passes are the same and follow the same welding directions (0°–90°–180°–270°–0°, Fig. 8(a)) in weld sequence-1. In the case of weld Sequence-2, the start point of weld pass 1 is at 0° and weld passes 2 and 3 are at 180°. It means that, in the case of weld pass 1, the direction of arc movement is 0°–90°–180°–270°–0°, whereas weld passes 2 and 3 are 180°–90°–0°–270°–180° (Fig. 8(b)). In Sequence-3 (Fig. 8(c)), the start and stop points of weld passes 1 and 2 are at 0° and 180°, respectively, and the corresponding arc directions of respective weld passes are 0°–90°–180°–270°–0° and 180°–90°–0°–270°–180°. In the case of weld pass 3, the start and stop points of the arc is the same as the weld pass 2 (180°), but the direction of welding changes opposite to weld pass 2 (180°–270°–0°–90°–180°). Firstly, the computation of the temperature history during welding and subsequent cooling was completed and then, the temperature field was applied to the mechanical model as a body force to perform the out-of-plane distortion analysis.

4. Results and discussion

4.1. Multi-pass weld thermal analysis of tube to pipe welding

In order to study the effect of weld thermal cycle on distortion generated during multipass weld deposition of the tube to pipe welding, two different locations, TC1 and TC2, were considered as shown in Fig. 2. At a given heat input and welding direction, the simulated and experimental weld thermal cycles under two different locations are shown in Figs. 10 and 11 respectively. In Fig. 10, it is observed that there are three peaks in the weld thermal cycle, confirming three weld passes involved in the tube to pipe component. Also, the maximum temperatures simulated at each weld pass in locations TC1 and TC2 differ from each other and are given in Table 3. This is primarily due to the fact that the location of TC1 is 5 mm away from the weld region and the location of TC2 is 15 mm away from the weld region.

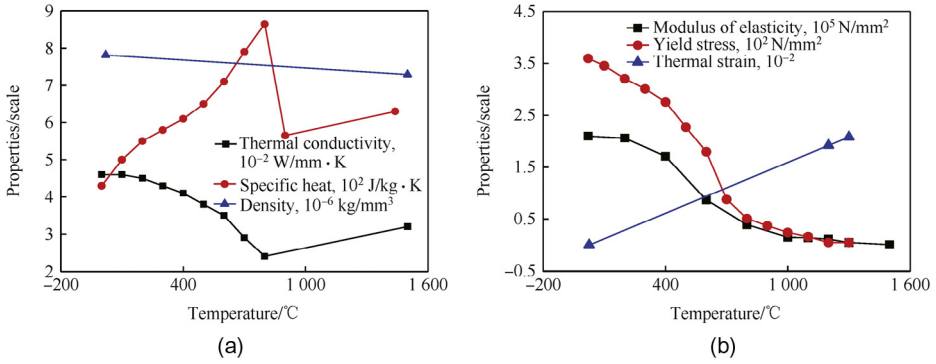

Fig. 7. The variation of properties with temperature. (a) Thermal properties and (b) mechanical properties.

Please cite this article in press as: R. Vetriselvan, K. Devakumaran, P. Sathiya, G. Ravichandran, Transient out-of-plane distortion of multi-pass fillet welded tube to pipe T-joints, Defence Technology (2016), doi: 10.1016/j.dt.2016.06.002

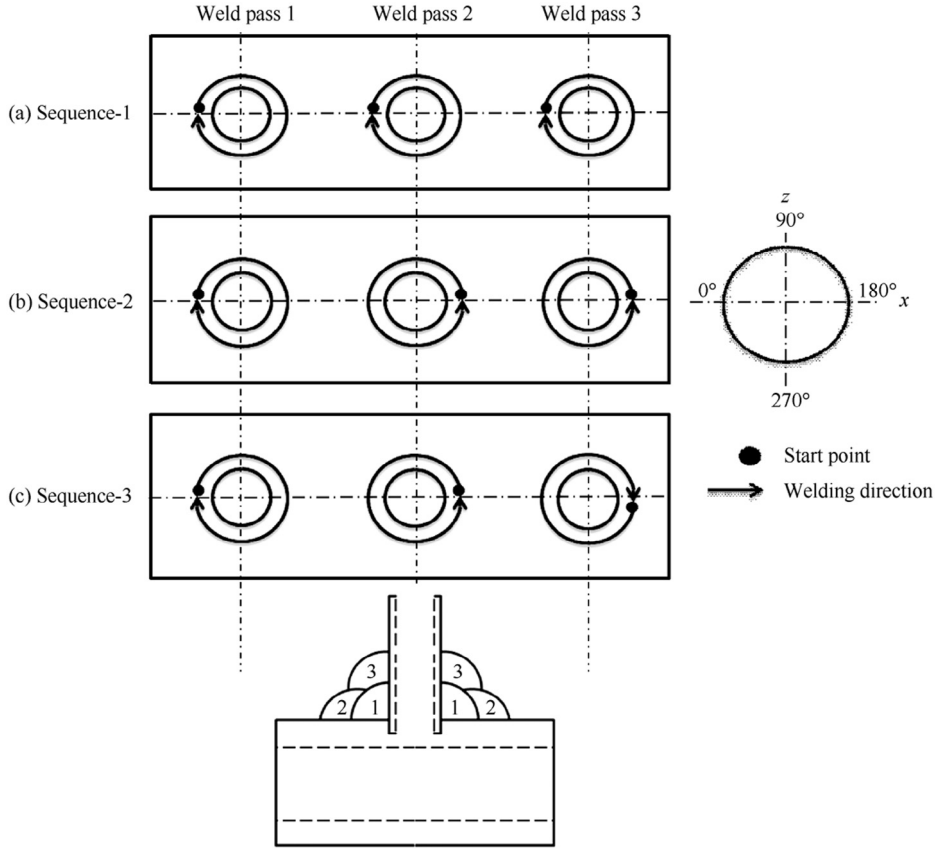

Fig. 8. The schematic diagram showing the three welding sequences considered for out-of-plane distortion analysis on multipass weld deposition of the tube to pipe component.

The variation in peak temperatures in TC1, between three weld passes, is attributed to the fact that weld pass 1 was carried out between the tube and the pipe with equal heat input distribution, whereas weld pass 2 was oriented between the pipe and the first weld pass. Hence, the tube receives less heat input comparatively and so peak 2 shows a lower temperature than peak 1. However, Weld pass 3 is oriented between the first weld pass and the tube and so peak 3 shows a higher temperature compared to peak 2. The maximum temperature recorded at TC1 is 1120 °C as the thermocouple is located in the tube nearer to weld.

In Fig. 11, it is observed that each weld pass shows two peak temperatures. It is due to the fact that the TC2 is heated twice as

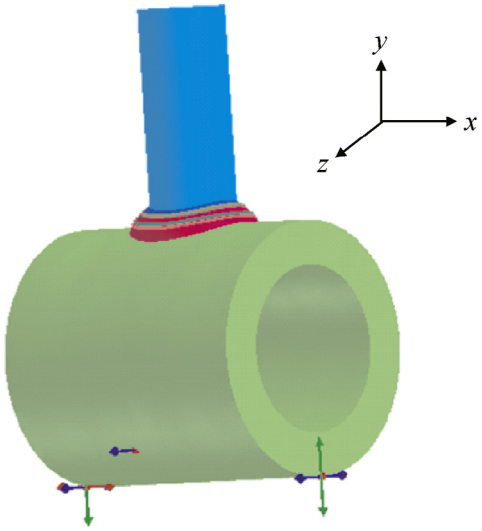

Fig. 9. The clamping condition considered to avoid the rigid body motions of the tube to pipe component.

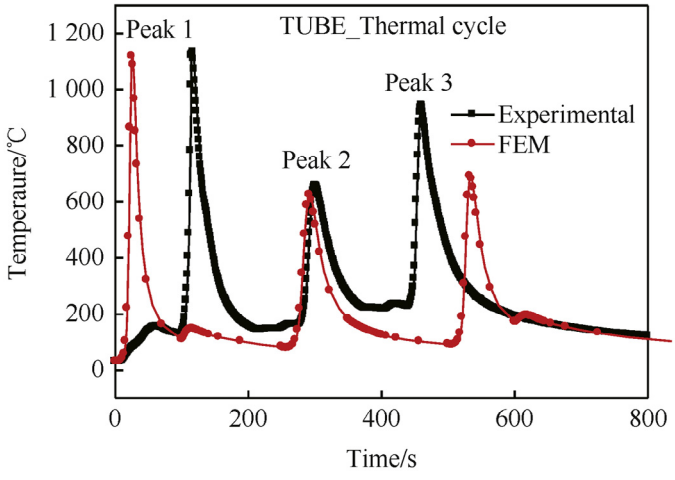

Fig. 10. Thermal cycle at a node in TC1.

Please cite this article in press as: R. Vetriselvan, K. Devakumaran, P. Sathiya, G. Ravichandran, Transient out-of-plane distortion of multi-pass fillet welded tube to pipe T-joints, Defence Technology (2016), doi: 10.1016/j.dt.2016.06.002

Table 3
The simulated and experimental peak temperatures at locations TC1 and TC2.

Nodal point locations	The simulated peak temperature obtained during different weld passes/°C		
	Weld pass 1	Weld pass 2	Weld pass 3
TC1	1120	620	693
TC2	Peak 1 = 188 Peak 2 = 264	Peak 1 = 253 Peak 2 = 327	Peak = 231 Peak = 279
	Experimental peak temperatures obtained during different weld passes/°C		
TC1	1134	657	944
TC2	Peak 1 = 123 Peak 2 = 197	Peak 1 = 237 Peak 2 = 286	Peak = 264 Peak = 284

start and stop points lie at the same location. These peaks are the characteristics of full circumferential welding. However, it is further observed that the peak 2 temperature is higher than the peak 1 temperature in all the three weld passes. During circumferential welding, the start point is once again reheated by the welding arc at the end of weld completion and therefore shows a higher temperature.

The cooling rate of each weld pass can be estimated in the region from its peak to 500 °C because this region is considered as a critical cooling condition in case of EN S355J2G3 [12]. It is observed that due to lower peak temperature, location TC2 shows lesser cooling rate than location TC1 irrespective of change in weld passes. Based on the results discussed above, the temperature contour plot obtained in the two different locations of TC1 and TC2 during multipass welding of tube to pipe at a given heat input and welding direction is shown in Fig. 12.

The peak temperatures obtained in the thermal analyses for experimental trials are also given in Table 3. It is found that both the FEM simulated and experimental curves follow a similar trend and the maximum temperatures reached during the welding are in agreement. It is due to the assumption of reasonable (material) thermal properties such as convection, heat transfer coefficients, co-efficient of thermal expansion and contraction, and thermal conductivity during the formulation of

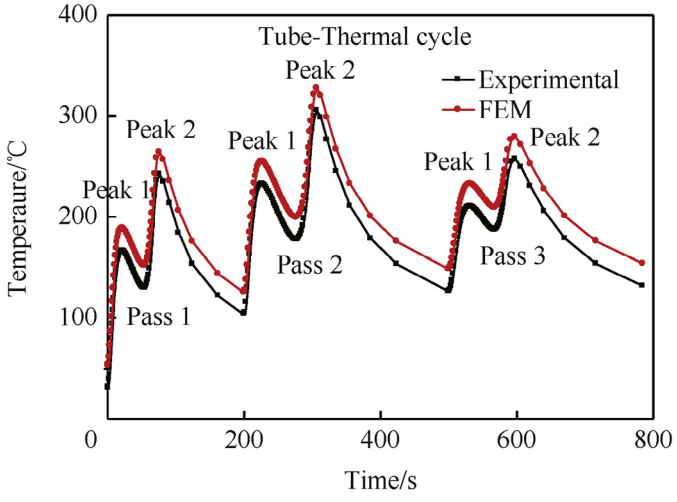

Fig. 11. The thermal cycle at a node in TC2.

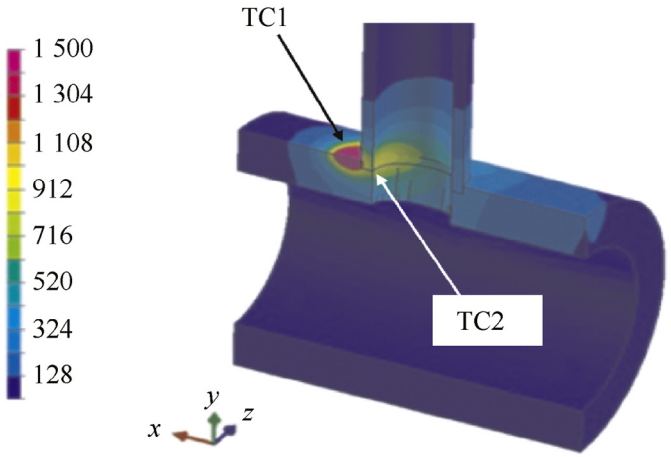

Fig. 12. The temperature contour of a tube to pipe set-on-type joint.

the thermal model. Similar material properties assumed for carbon steel in the study yielded good results elsewhere [14].

The deviation of maximum temperature reached by the FEM model and experimental result is 10%. It can also be noted that there is an offset between FEM and experimental curves in time (x-axis). It is attributed to two reasons majorly.

1) The position of the thermocouple in the FEM model is at the exact location, whereas identifying the same location in the experimental trial is arbitrary and has a slight offset.
2) The welding process used for the investigation is SMAW. The manual welding time between different weld passes is not uniform in the case of the experimental trial. This causes a slight time offset in the x-axis, whereas the FEM simulations follow a uniform time gap between the weld passes. Due to this time shift in the x axis, the FEM and experimental curves are slightly shifted.

4.2. Out-of-plane distortion analysis of tube to pipe welding

The transient out-of-plane distortion simulated during multipass weld deposition of the tube to pipe welding at a given weld sequence-1 is shown in Fig. 13. From the figure, it is observed that an increase in the number of weld passes increases the out-of-plane distortion in both directions (x and z) of the tube. This is primarily because an increase of quantum of weld metal deposition results in the accumulation of heat input giving rise to weld metal contraction. It is also observed that out-of-plane distortion in the x direction is higher than that in the z direction because the overall heat input in x direction is higher than the z direction. The excess heat input in the x direction is contributed by the weld start and stop points of all the three weld passes, whereas in the z direction there is no such start and stop points in Sequence-1. Similarly, the out-of-plane distortion in the z direction is the effect of time lag associated with the welding direction between different weld passes. Therefore, it is inferred that out-of-plane distortion in the z direction is primarily influenced by the welding direction, whereas distortion in the x direction is influenced by heat input due to the arc start and stop points in the same location.

Please cite this article in press as: R. Vetriselvan, K. Devakumaran, P. Sathiya, G. Ravichandran, Transient out-of-plane distortion of multi-pass fillet welded tube to pipe T-joints, Defence Technology (2016), doi: 10.1016/j.dt.2016.06.002

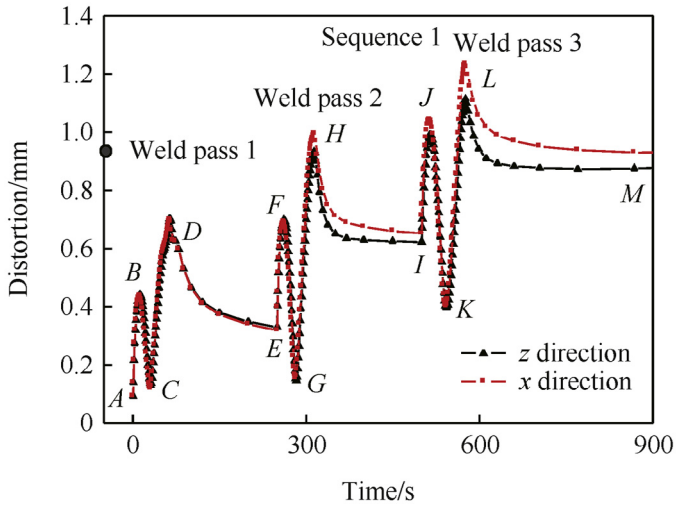

Fig. 13. The effect of weld Sequence-1 on out-of-plane distortion under multipass weld deposition of tube to pipe welding.

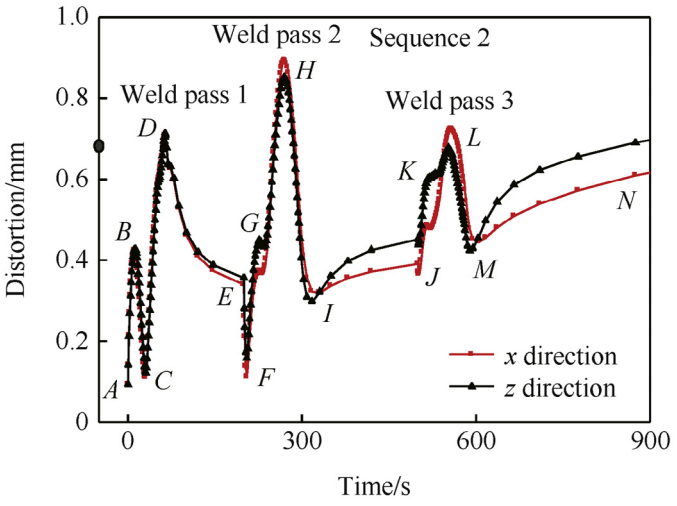

Fig. 14. The effect of weld Sequence-2 on out-of-plane distortion under multipass weld deposition of tube to pipe welding.

In order to establish a clearer understanding about the effect of welding sequence on out-of-plane distortion induced during tube to pipe welding, the trends of tube movements around the circumferential welding of each weld pass were analyzed. In Fig. 11, it is observed that there are two different peaks in each weld pass. These peaks indicate the out-of-plane distortion behavior during heating and cooling cycles of circumferential fillet welding of the tube to pipe. Points *A*, *E* and *I* are the start points of each weld pass. Curves *A–B*, *E–F* and *I–J* represent the heating cycle of weld deposition from 0° to 180° of weld passes 1, 2 and 3, respectively, and corresponding cooling cycles are *B–C*, *F–G* and *J–K* respectively. During circumferential welding, the curve (*A–B*, *E–F* and *I–J*) moving to a positive direction indicates that expansion takes place during the heating cycle. The curve (*B–C*, *F–G* and *J–K*) moving to the negative direction indicates the contraction that takes place during the cooling cycle. After that, the arc moves to the opposite direction (180°–0°) during the circumferential welding. Curves *C–D*, *G–H* and *K–L* and *D–E*, *H–I* and *L–M* are the heating and cooling cycles from 180° to 0° of weld passes 1, 2 and 3 respectively. As in the case of weld deposition from 0° to 180°, it is observed that the expansion and contraction take place during heating and cooling cycles respectively. However, the magnitude of distortion generated in the direction 180°–0° is higher in comparison to that of the direction 0°–180°. This is due to the effect of the time lag involved in the welding direction of weld sequence-1.

The effect of weld sequence-2 on out-of-plane distortion induced during multipass weld deposition of the tube to pipe fabrication is shown in Fig. 14. It is observed that the increase of weld passes increases the distortion in both directions. In welding sequence-2, weld pass 2 showed a negative distortion trend during heating *E–F* when the weld deposition was from 0° to 180°. This is in contrast to Sequence-1 of weld pass 2. This behavior primarily occurred due to the shifting of the starting point of the arc to 180°. In Fig. 14, it is further observed that a little shift in distortion trend is observed in points *G* and *K* because of the time lag effects due to the change in welding direction. It can also be noted that the out-of-plane distortion induced in the *x* direction is lower than the *z* direction especially at weld pass 3, which is in contrast to sequence-1 (Fig. 13) due to the effect of the same weld direction involved in weld passes 2 and 3 than the effect of the arc start and stop points. This behavior resulted in the reduction of out-of-plane distortion in both *x* and *z* directions compared to Sequence-1.

The effect of weld sequence-3 on out-of-plane distortion induced during multi-pass weld deposition of the tube to pipe fabrication is shown in Fig. 15. Among the three weld sequences, sequence-3 induces the lowest distortion in both directions. This is primarily due to the balancing effect of heat input due to the start and stop points and welding direction. In sequence 3, the welding direction of each weld pass is entirely different from each other and accordingly balances the heat

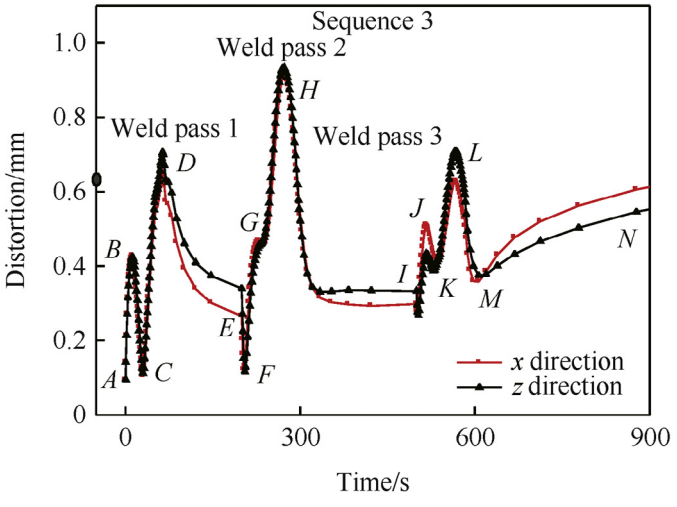

Fig. 15. The effect of weld Sequence-3 on out-of-plane distortion under multipass weld deposition of tube to pipe welding.

Please cite this article in press as: R. Vetriselvan, K. Devakumaran, P. Sathiya, G. Ravichandran, Transient out-of-plane distortion of multi-pass fillet welded tube to pipe T-joints, Defence Technology (2016), doi: 10.1016/j.dt.2016.06.002

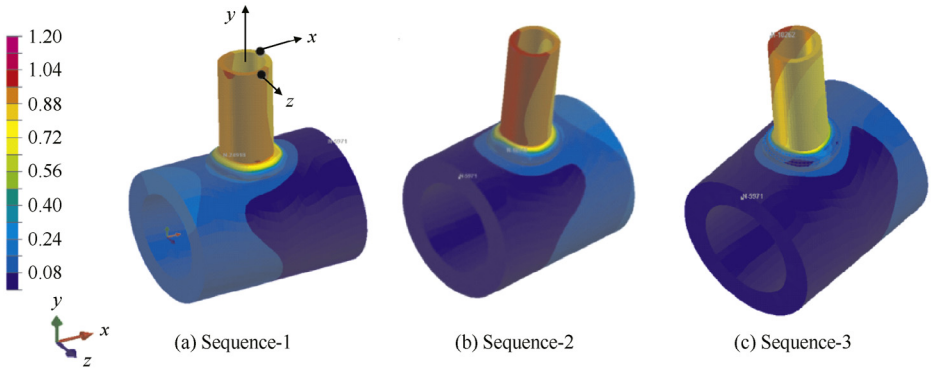

Fig. 16. The FEM-simulated displacement contour for three weld sequences.

Table 4
The experimental validation of FEM simulated out-of-plane distortion.

Weld sequence (distortion direction)	Distortion/mm		
	FEM	Experiment	Deviation/%
Sequence-1-*x*	0.929	1.10	14.03
Sequence-1-*z*	0.873	1.0	15.04
Sequence-2-*x*	0.609	0.72	15.41
Sequence-2-*z*	0.690	0.78	11.53
Sequence-3-*x*	0.605	0.72	12.00
Sequence-3-*z*	0.546	0.64	14.60

input during circumferential welding of the tube results in the reduction of out-of-plane distortion. Based on the above discussions, it is well understood that the welding sequence plays a major role in minimizing the out-of-plane distortion induced during circumferential welding of the tube to pipe component.

After weld metal deposition at the 1500th second (at this time, the weld metal deposition reached to room temperature ensures the complete contraction takes place during the cooling cycle), the steady state contours of different weld sequences 1, 2 and 3 are shown in Fig. 16(a)–(c). This contour shows the out-of-plane distortion occurred on the tube to pipe component after completion of all weld passes. In Fig. 16, it is observed that the tube movements due to circumferential welding under different weld sequences are entirely different from each other because of the change of welding direction and weld start/stop points as explained earlier.

The simulated and experimentally measured out-of-plane distortion data are presented in Table 4. The steady state out-of-plane distortion magnitudes of FEM and experimental analyses are validated and are shown in Figs. 17 and 18. The FEM predicted and experimentally measured values of out-of-plane distortion during tube to pipe welding under different weld sequences and directions are in agreement with the deviation of around 15%. Compared to thermal analysis, mechanical analysis has 5% more deviation. This could be attributed to the manual error involved in the distortion measurement. Based on the FEM and experimental results, the suitable welding sequences and directions were established for the tube to pipe component.

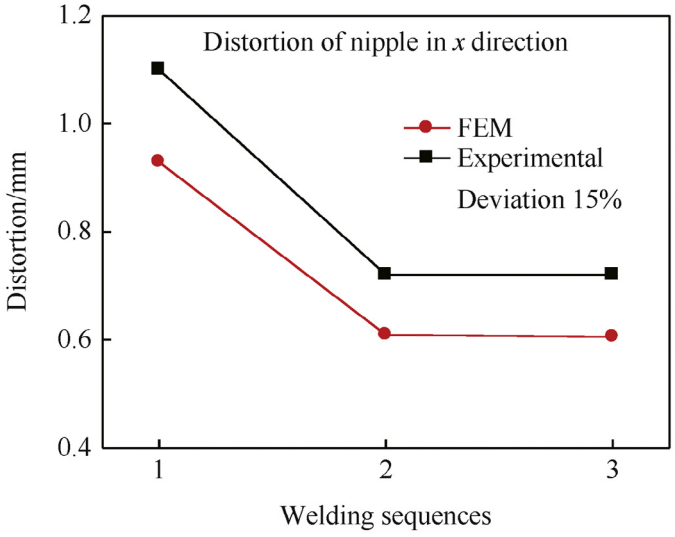

Fig. 17. The steady state distortion magnitudes of FEM and experimental results in *x* direction.

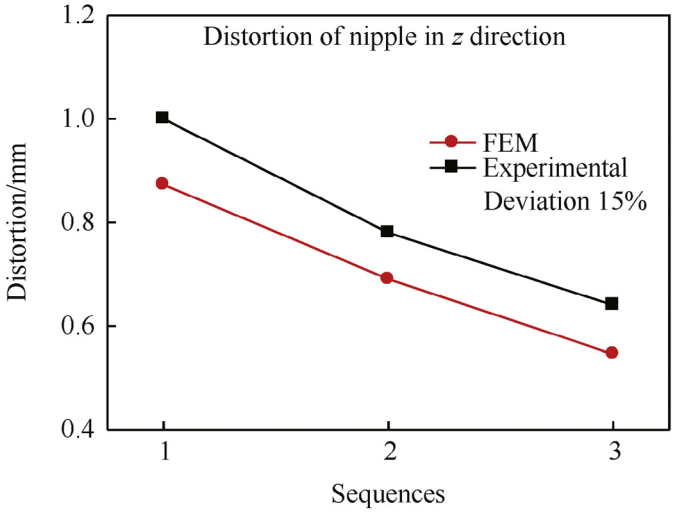

Fig. 18. The steady state distortion magnitudes of FEM and experimental results in *z* direction.

Please cite this article in press as: R. Vetriselvan, K. Devakumaran, P. Sathiya, G. Ravichandran, Transient out-of-plane distortion of multi-pass fillet welded tube to pipe T-joints, Defence Technology (2016), doi: 10.1016/j.dt.2016.06.002

5. Conclusion

The FEM model was used to study the out-of-plane distortion during multi-pass circumferential fillet welding of the tube to pipe component under three different welding sequences and directions. The FEM model was validated through experiments. Based on the study, the control of out-of-plane distortion was explored and the following conclusions were made.

1) The thermal analysis was carried out using thermal cycles captured at two locations around the tube and it was observed that the distortion trend was influenced by thermal cycle. The change in welding direction causes the significant change in thermal cycle thereby out-of-plane distortion trend is changed in case of circumferential fillet welding.
2) The out-of-plane distortion increases when all the three weld passes follow the same circumferential direction around the tube. This is due to the combined effect of heat input due to the same start and stop points and welding direction of the arc. However, the out-of-plane distortion decreases when all the three weld passes follow different circumferential directions to each other around the tube. This is due to the balancing of heat effects of weld passes due to change in welding direction.
3) The multi-pass circumferential fillet welding of the tube to pipe induces out-of-plane distortion of the tube. The heat input due to weld start and stop points influences the out-of-plane distortion in the x direction. The welding direction and associated time lag effects between different weld passes influence the out-of-plane distortion in the z direction.
4) Experimental results confirm the mechanism of out-of-plane distortion explored by FEM analysis, hence the suitable welding procedure was established for the tube to pipe component.

Acknowledgment

The authors wish to express their sincere thanks to M/s Bharat Heavy Electricals Ltd, Tiruchirappalli, India for providing permission to carry out this research work at their works.

References

[1] Chul KY. Production mechanism of out-of-plane deformation in fillet welding. Trans JWRI 1998;27(2).
[2] Jung GH, Tsai CL. Fundamental studies on the effect of distortion control plans on angular distortion in fillet welded T-joints. Weld J 2004; 213s–223s.
[3] Rui W, Sherif R, Hisashi S, Hidekazu M, Zhang J. Numerical and experimental investigations on welding deformation. Trans JWRI 2008; 79–90.
[4] Wang J, Rashed S, Murakawa H, Luo Y. Numerical production and mitigation of out-of-plane welding distortion in ship panel structure by elastic FE analysis. Mar Struct 2013;34:135–55.
[5] Vetriselvan R, Raju N, Ravichandran G, Suresh S. Analysis of angular distortion in stainless steel T joint using FEM. WRI J 2011;32: 29–38.
[6] Deng D, Murakawa H, Liang W. Numerical simulation of welding distortion in large structures. Comput Methods Appl Mech Eng 2007; 4613–27.
[7] Ravichandran G, Raghupathy VP, Ganesan N, Krishnakumar R. Prediction of axis shift distortion during circumferential welding of thin pipes using the finite element method. Weld Res Suppl 1997; 39s–55s.
[8] Dar NU, Qureshi EM, Hammouda MMI. Analysis of weld induced residual stresses and distortions in thin walled cylinders. J Mech Sci Technol 2009;23:1118–31.
[9] Yu C-L, Chen Z, Wang J, Yan S, Yang L-C. Effect of weld reinforcement on axial plastic buckling of welded steel cylindrical shells. J Zhejiang Univ Sci A 2012;2012(2). ISSN 1862-1775 (online).
[10] Sagalevich VM, Shvetsov VA, Baumana NE. Distortion in welding circumferential seams in thin walled shells. In: Welding production. Cambridge: The Welding Institute; 1970.
[11] Vetriselvan R, Sudharsanam V, Raju N, Ravichandran G. Analysis of angular distortion in header to nipple welding using FEM. In: International symposium on joining of materials. Tiruchirappalli: IWS; 2012.
[12] Vetriselvan R, Sathiya P, Ravichandran G. Characterization of transient out-of-plane distortion of nipple welding with header component. J Manuf Process 2015;67–72.
[13] Sysweld. Manual. France: ESI; 2014.
[14] Dialami N, Chiumenti M, Agelet de Scracibar C, Cervera M. A strategy for the numerical simulation of metal deposition and multipass welding process. In: International conference on computational plasticity. Barcelona: CIMNE; 2009.
[15] Goldak J, Chakravarti A, Bibby M. A double ellipsoidal finite element model for welding heat sources. IIW Doc 212-603-85. 1985.

Please cite this article in press as: R. Vetriselvan, K. Devakumaran, P. Sathiya, G. Ravichandran, Transient out-of-plane distortion of multi-pass fillet welded tube to pipe T-joints, Defence Technology (2016), doi: 10.1016/j.dt.2016.06.002